Review of Scientific Instruments

Operando reaction cell for high energy surface sensitive x-ray diffraction and reflectometry

Cite as: Rev. Sci. Instrum. **93**, 073902 (2022); https://doi.org/10.1063/5.0098893
Submitted: 13 May 2022 • Accepted: 16 June 2022 • Published Online: 06 July 2022

R. Gleißner, E. E. Beck, Simon Chung, et al.

Review of Scientific Instruments ARTICLE scitation.org/journal/rsi

Operando reaction cell for high energy surface sensitive x-ray diffraction and reflectometry

Cite as: Rev. Sci. Instrum. 93, 073902 (2022); doi: 10.1063/5.0098893
Submitted: 13 May 2022 • Accepted: 16 June 2022 •
Published Online: 6 July 2022

R. Gleißner,[1,2] E. E. Beck,[1,2] Simon Chung,[1] G. D. L. Semione,[1,2,a)] N. Mukharamova,[1] G. Gizer,[3] C. Pistidda,[3] D. Renner,[1] H. Noei,[1] V. Vonk,[1] and A. Stierle[1,2,b)]

AFFILIATIONS

[1] Centre for X-ray and Nano Science CXNS, Deutsches Elektronen-Synchrotron DESY, Notkestraße 85, 22607 Hamburg, Germany
[2] Fachbereich Physik, Universität Hamburg, Jungiusstraße 9, 20355 Hamburg, Germany
[3] Institute of Hydrogen Technology, Materials Technology, Helmholtz-Zentrum hereon GmbH, Max-Planck-Straße 1, 21502 Geesthacht, Germany

[a)] **Current address:** MAPEX Core Facility for Materials Analytics, MAPEX Center for Materials and Processes, University of Bremen, 28334 Bremen, Germany.
[b)] **Author to whom correspondence should be addressed:** andreas.stierle@desy.de

ABSTRACT

A proof of concept is shown for the design of a high pressure heterogeneous catalysis reaction cell suitable for surface sensitive x-ray diffraction and x-ray reflectometry over planar samples using high energy synchrotron radiation in combination with mass spectrometry. This design enables measurements in a pressure range from several tens to hundreds of bars for surface investigations under realistic industrial conditions in heterogeneous catalysis or gaseous corrosion studies.

I. INTRODUCTION

Over the last few decades, the development of machinery that combines the advantages of traditional surface science methods and *operando* reaction conditions advanced rapidly. Tools such as ambient pressure x-ray photoelectron spectroscopy[1,2] and ambient pressure scanning tunneling microscopy[3–5] demonstrated in a variety of successful experiments that it is possible to achieve an atomistic understanding of the contributing surfaces and reaction mechanics in non-vacuum conditions. Hard x-ray scattering can also address the surface structure, is not hindered by non-vacuum conditions, and can penetrate chamber walls.[6] Several sample environments have been developed for surface sensitive x-ray diffraction[7,8] or high pressure x-ray reflectivity.[9–11] In many cases, the industrially relevant reaction pressures can be several orders of magnitude higher than ambient pressure, e.g., the synthesis of methanol and hydrogenation of CO_2 over $Cu/ZnO/Al_2O_3$ catalysts utilize temperatures of 470–520 K and pressures of 50 bars and above in industrial plants.[12] In order to completely overcome the pressure gap between ultra-high vacuum and realistic reaction conditions for surface science investigations, especially for catalysis under gas flow, new instruments need to be created.

Fixed-bed cells utilizing powder samples have previously been designed for the use of x-ray absorption spectroscopy and x-ray diffraction measurements to obtain information of the structure of the catalyst while simultaneously probing the gas environment under *operando* conditions.[13–18] While certain knowledge can be extracted from powder diffraction experiments, surface sensitive x-ray diffraction is a more elaborate tool and better suited to achieve a detailed understanding of the catalyst–surface interactions.[19] It utilizes single crystalline samples that can be covered with nanoparticles and adlayers or be otherwise conditioned to mimic a specific catalytic interplay.[7] Information about surface roughness, surface reconstruction effects, and defects and the strain, size, orientation, and lattice spacing of the nanoparticles or adlayers can be acquired for the specific single crystal facet under investigation.[7] Additionally, x-ray reflectometry can be performed in this measurement geometry, which yields information about the layer thickness, interface roughness, and the electron density profile at the surface, e.g., nanoparticle height and surface coverage.

A variety of advancements in the combination of surface sensitive x-ray diffraction with other experimental methods were developed in the last few decades, such as ellipsometry,[20] x-ray photoelectron spectrometry,[21] surface optical reflectance and planar laser induced fluorescence,[22] or the use of electrochemically integrated flow cells,[23] pioneering an intertwined understanding from different points of view.

In this article, we present the design of a high pressure *operando* reaction cell for high energy surface sensitive x-ray diffraction (HESXRD) and x-ray reflectometry (XRR) on single crystalline samples, thin films, and supported nanoparticles. Measurements were performed utilizing pressures of up to 50 bars of Ar, H_2, CO, and CO_2 with sample temperatures of up to 600 K. While the pressure and temperature limits of the capillary itself were not tested in this proof-of-concept study, similar cell geometries point toward pressure ranges of up to several hundred bars.[24]

II. SETUP DESIGN

The main concept of the instrument is based on a single crystalline Al_2O_3 capillary, which acts as both the gas pressure cell and the window for hard x rays. This material was chosen as it has proven to withstand pressures of up to 700 bars at 770 K[24] and is sufficiently transmissive for a high energy synchrotron beam with, e.g., $h\nu = 73$ keV (see Fig. 1). With the utilized cell geometry, the x-ray beam passes through 1 mm Al_2O_3 twice as the incident beam and after reflection/diffraction from the sample, losing 15% of its intensity due to absorption and scattering with the capillary. The usage of, e.g., steel as a capillary material would decrease the x-ray transmission through the cell significantly for photon energies below 100 keV and would, furthermore, lead to a high number of artifacts originating from its polycrystalline domains. Rather than utilizing an amorphous or polycrystalline cell material, which increases the overall background in the detector images, the goal is to identify and individually block the Bragg peaks that are diffracted off the single crystalline capillary. Another important advantage is the low thermal conductivity of oxide-based capillaries compared to metals, which enables the use of polymer ferrules as gaskets of the capillary during measurements at elevated temperatures.

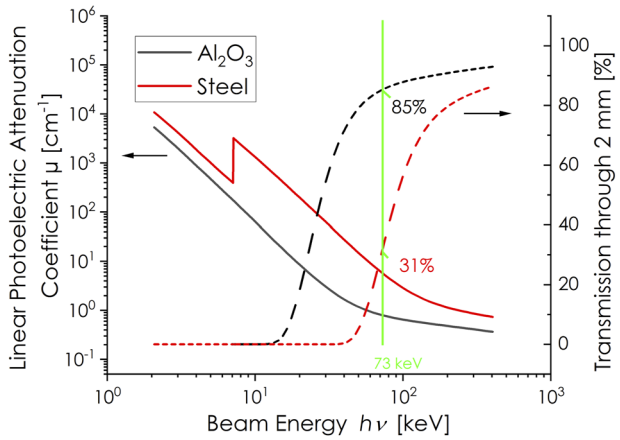

FIG. 1. The linear photoelectric x-ray attenuation coefficient μ (left axis)[25] and transmission I/I_0 through a 2 mm material (right axis) of Al_2O_3 (black) as utilized for the experimental reaction cell compared to steel ($Fe_{99}C_1$, red).

A. Reaction cell

The experimental design features three assemblies: the gas supply system, the reaction cell assembly as well as the pressure regulator, and the gas analysis section. They are separated by flexible tubing that allows the reaction cell assembly to be mounted on a tower of goniometers and linear translators. The reaction cell itself consists of a single crystalline Al_2O_3 capillary with two inner diameters of 2 and 4 mm, intersecting at the center of the capillaries' full length [Fig. 2(a)]. Thus, an edge is presented where a round Al_2O_3 "crown spacer" [Fig. 2(c)] is introduced through the larger opening. It serves three purposes as (1) it directs the gas flow around the sample, preventing the capillary to be clogged; (2) it accounts for the transition angle at the intersection of the two inner diameters with a phase at the bottom of the crown spacer, which prevents rocking motions during the measurements; and (3) it is an inexpensive, easily exchangeable part to account for issues during the iterative design optimization and to easily tune, e.g., the height of the sample inside the reaction cell. This height is of importance as the Al_2O_3 capillary usually has at the intersection of the two inner diameters a higher impurity density, polycrystallinity, and other defects due to the manufacturing process. A crown spacer and sample are introduced into the capillary by sliding them subsequently onto the internal step prior to mounting the capillary into the holding stage. The sample was found to be placed sufficiently stable for all necessary angular and translational movements of the goniometer stage in a grazing incidence beam geometry as the gas flow additionally presses the sample and crown spacer against the internal capillary step.

The sample geometry requires diameter D_S and height H_S that fulfill $\sqrt{H_S^2 + D_S^2} > D_C$, with D_C being the larger inner diameter of the capillary in order to avoid flipping of the sample to its side. A minimum height H_S of 1.0 mm for metal and 1.5 mm for oxide samples is recommended if side slits are used for mounting in, e.g., UHV systems in order to avoid bending or breaking of the sample surface.

For the connection to the gas supply, Vespel® ferrules are utilized to seal against the hot, high pressure, potentially corrosive, and

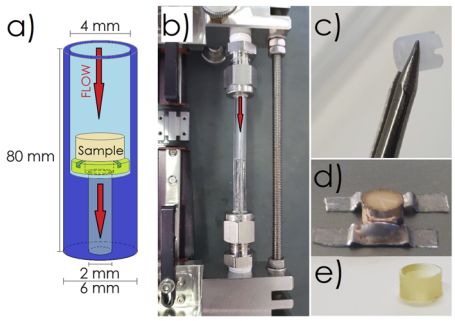

FIG. 2. Reaction cell design. (a) Scheme of the capillary with two inner diameters of 2 and 4 mm, the crown spacer (green), and the single crystal sample. (b) Reaction cell mounted in the holding stage. (c) Al_2O_3 crown spacer in detail. Cylindrical Cu (d) and ZnO (e) samples of 3.5 mm diameter.

toxic gas feed. The top and bottom connections [Fig. 2(b)] can be linearly translated to adjust for different capillary lengths and for capillary mounting purposes. The rigidity of the frame against the high pressures is ensured by connection screws (right side), which are affixed after the mounting of the capillary. An excess flow valve upstream and a check valve downstream from the capillary shut off the gas supply in the case of capillary rupture.

A thermocouple can be introduced from the bottom of the capillary frame through a Vespel ferrule sealed feedthrough, upward inside the 2 mm inner diameter of the capillary contacting the backside of the sample. If the sample is metallic, the thermocouple could be welded directly to the sample to allow for the temperature measurement during the experiment. For insulating samples, it is recommended to run a temperature calibration prior to the experiment as the thermocouple may lose contact during heating.

B. Gas supply system and gas analysis

The technical scheme of the gas handling system is depicted in Fig. 3. In this configuration, it utilizes H_2, Ar, CO, and CO_2 as feed gases as used in a wide variety of experiments, e.g., the water gas shift reaction, methanol, or Fischer–Tropsch synthesis.

The Ar, H_2, and CO gas lines feature mass flow controllers (Bronkhorst® EL-FLOW Select), while the CO_2 line utilizes a Coriolis mass flow controller (Bronkhorst mini CORI-FLOW) as required by the low condensation pressure of about 50 bars at room temperature (triple point at 31.0 °C and 73.9 bars). For precise operation, the latter must be mounted on a vibration suppressing stand. The CO gas supply requires the use of a carbonyl trap (CT; PALL Mini GasKleen®) for which we utilized an active material gas purifier. It is important to note that the carbonyl trap should be mounted upstream from the H_2 and CO_2 supply lines to avoid degradation of its active material. Two back pressure regulators (BPR; Bronkhorst EL-PRESS) keep the reaction cell at the desired experimental pressure while regulating the pressure in between them to 1 bars(g), from which a sample gas stream is leaked trough a needle valve into the quadrupole mass spectrometer (QMS) or gas chromatograph (GC).

For mass spectrometry, long dwell times of the gas feed on the sample surface are needed to account for the small surface area of single crystals compared to powder samples. Thus, a flow rate range of 0.9–45 ml(n)/min for each individual mass flow controller was chosen. The operation of the utilized mass flow controllers requires differential pressures of minimum 13 bars(g) and maximum 40 bars(g). Thus, for pressures above 40 bars(g), either a step-wise increase of the inlet and outlet pressure or a pre-pressurization from the bypass gas supply is needed.

Bypasses and a vacuum pump were integrated to evacuate and flush all gas lines in order to remove contamination and residual moisture. Depressurization to about ambient pressures via a gradual relief valve bypassing the pump is necessary prior to its operation.

C. Heating and temperature

To increase the sample temperature to the desired experimental conditions, an external heat gun is utilized that directs a flow of hot air onto the capillary. In this proof-of-concept study, a Steinel® HG 2320E heat gun with an attached metal cone to focus the air flux was used, which was able to deliver hot air between 350 and

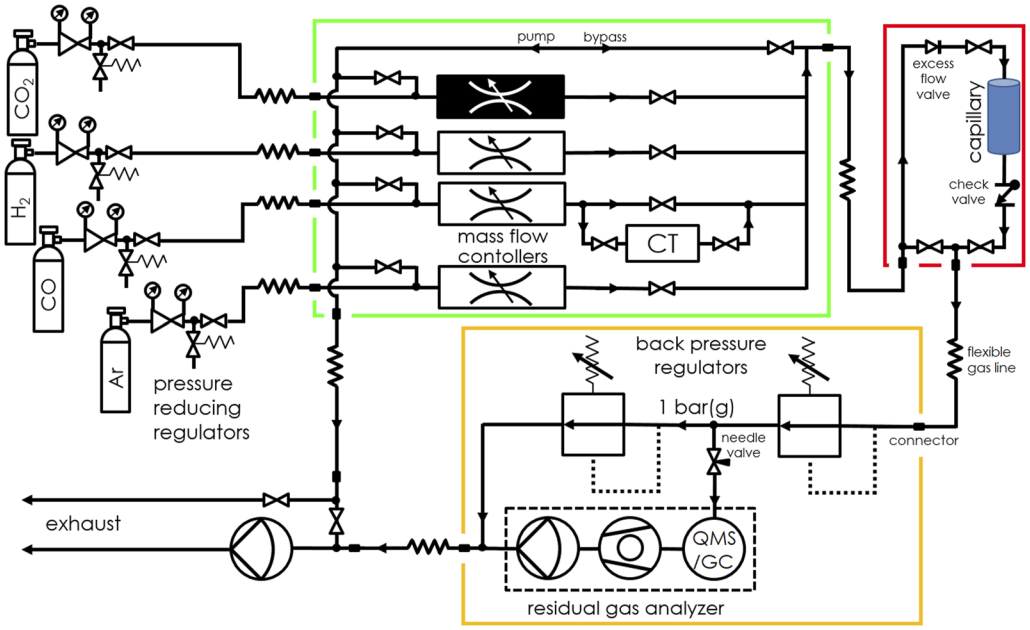

FIG. 3. Technical scheme of the gas handling system (green square), the reaction cell assembly (red square) as well as the pressure regulator, and gas analysis section (orange square) of the high pressure HE-SXRD experimental setup.

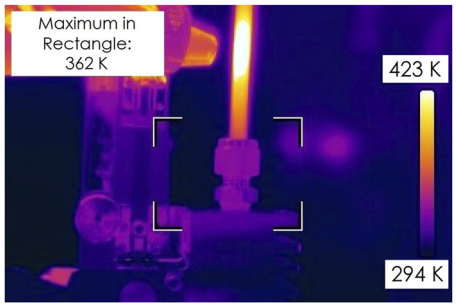

FIG. 4. Infrared camera image of the capillary with a heat gun temperature of T_{gun} = 820 K and 50 bars Ar at 45 ml(n)/min, achieving a sample temperature of 575 K.

920 K with an air flux of 150 or 500 l/min. It should be freestanding and not mounted attached to the diffraction setup in order to avoid the blockage of the x-ray beam pathway. The temperature of the sample is rather influenced by the geometry of the heat gun setup than by changes of the flow rate or pressure of the gas feed inside the capillary. Thermal expansion effects that lead to the misalignment of the sample surface with respect to the x-ray beam are easy to adjust for although significant compared to the narrow beam sizes of typically 2–3 μm for high energy grazing incidence XRD experiments.[26]

The length of the capillary plays an important role in the safety concept of the experimental cell as the Vespel ferrules exhibit a maximum operation temperature of 620 K. In order to achieve sample temperatures of 600 K and beyond, the Al_2O_3 capillary surpasses the maximum operation temperature of the ferrules at the height of the sample. With a distance of 4 cm to the ferrules, the low thermal conductivity[27] of the Al_2O_3 capillary of 50 W m^{-1} K^{-1} and the heat exchange with the gas inside and outside of the capillary are sufficient enough to achieve temperatures within the operation limits of the ferrules, as shown in Fig. 4.

III. EXAMPLE MEASUREMENTS

Figure 5 displays high energy x-ray diffraction data of a Cu(110) single crystal at room temperature and 30 bars H_2 after heating to 520 K under 30 bars H_2. Figure 6 depicts $\Delta q_{x,y}$ scans in reciprocal space horizontally across the minima of the three crystal truncation rods (CTRs)[30,31] shown in Fig. 5. The acquisition of signal data at these points in reciprocal space serves as a proof of concept that the designed reaction cell is suitable for these kinds of measurements. The presence of the signal indicates that the Cu(110) surface stays atomically smooth at 30 bars H_2 exposure.

Besides the Cu CTRs on the detector, numerous intense artifacts are visible that arise from the Al_2O_3 capillary. The "random" placement of these features arises due to the transmission twice through the Al_2O_3 capillary wall although it also indicates that the capillary was fairly polycrystalline at the height of the sample surface. We are confident that the observed artifacts in the HE-GIXRD images can be largely reduced by the use of a capillary of higher quality, i.e., larger grain sizes to a point where they can be individually blocked by beam stops on the 2D detector. Since the unsatisfying quality is a result of the fusing process of two separate capillaries,

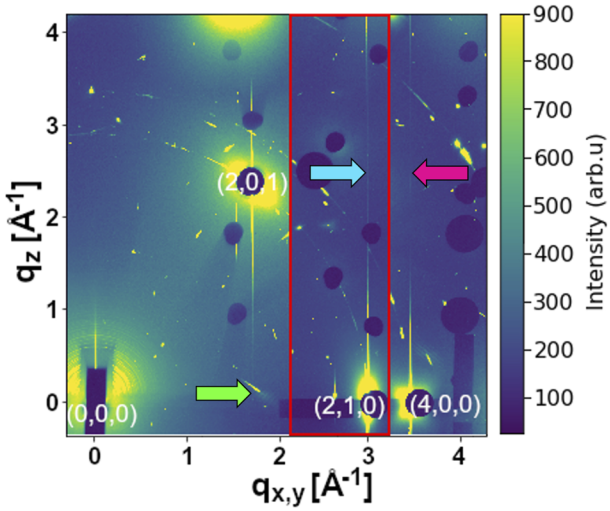

FIG. 5. High energy surface sensitive x-ray diffraction measurement of a Cu(110) surface at room temperature and 30 bars H_2 after heating to 520 K under 30 bars H_2 displayed in reciprocal space. The image shows the maximum pixel intensity over a range of ω = 20° around the (2,0) and (4,0) CTRs and around the (2,1) CTR (red outlined inset). The white labels indicate the Cu Bragg peaks in surface coordinates.[28] An x-ray photon energy of $h\nu$ = 67 keV with a grazing incidence angle of θ_i = 0.06° at 3.4 keV bandwidth and a Varex imaging XRD 4343CT detector[29] were utilized. The green, magenta, and cyan arrows point at CTR intensity minima for which line scans are depicted in Fig. 6.

this may be circumvented by alternatively boring holes with 2 and 4 mm inner diameters into a solid Al_2O_3 cylinder. In addition, the use of a higher crown spacer can offset the samples' surface away from the capillary region of poor quality.

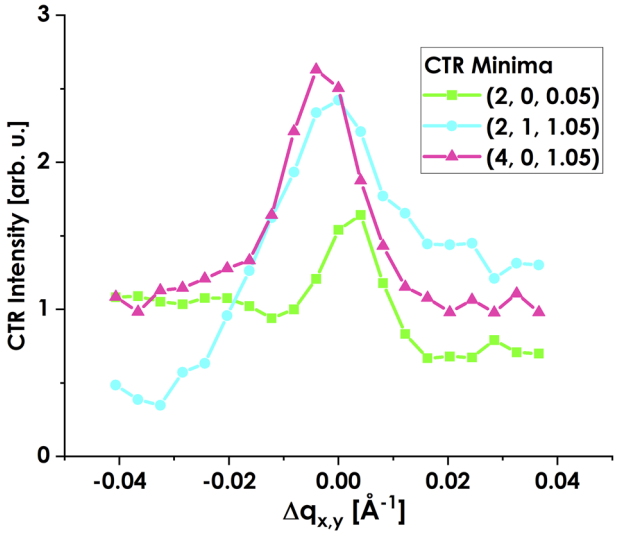

FIG. 6. $\Delta q_{x,y}$ line scans in reciprocal space horizontally across the CTRs of the Cu(110) sample at 30 bars H_2 and room temperature. The coordinates in the legend correspond to h, k, and l values in Cu(110) surface coordinates, as depicted in Fig. 5. The line scans were chosen at l = 0.05 and l = 1.05 to accommodate for the influence of the sample horizon and signals originating from layer occupation factors of the surface atoms that result in a local maximum at integer values of l.

IV. CONCLUSIONS

This study shows a proof of concept for an *operando* reaction cell for surface sensitive high-energy grazing-incidence x-ray diffraction and reflectometry utilizing single crystal samples or samples with mirror-like surfaces. The test measurements were performed up to a maximum of 50 bars Ar and a sample temperature of 600 K, yet higher values are expected to be achievable. The use of a gas supply system allows for the use of gas feeds containing mixtures of Ar, H_2, CO, and CO_2. Once capillaries of satisfying crystal quality have been obtained, stability stress tests will reveal which catalytic systems, reactions, or surface mechanisms of interest come into question to be studied in this conceptional setup. The first experiments demonstrate that the surface signal from a Cu(110) single crystal at 30 bars H_2 pressure can be extracted, despite the high background from the capillary. As the operational range of surface science techniques extends to several tens to hundreds of bars, surface studies of model systems under true industrial conditions become feasible.

ACKNOWLEDGMENTS

We acknowledge DESY (Hamburg, Germany), a member of the Helmholtz Association HGF, for the provision of experimental facilities. Parts of this research were carried out at PETRA III, P21 beamline. We acknowledge support from the Helmholtz Foundation through the Helmholtz-Lund International Graduate School (HELIOS, Grant No. HIRS-0018). We also acknowledge the Helmholtz Energy Materials Characterization Platform (HEMCP) for instrumental support.

AUTHOR DECLARATIONS

Conflict of Interest

The authors have no conflicts to disclose.

Author Contributions

R. Gleißner: Conceptualization (equal); Data curation (equal); Formal analysis (lead); Investigation (lead); Methodology (lead); Visualization (lead); Writing – original draft (lead); Writing – review & editing (equal). **E. E. Beck:** Investigation (supporting); Methodology (supporting). **Simon Chung:** Investigation (supporting); Writing-review-editing (supporting). **G. D. L. Semione:** Investigation (supporting). **N. Mukharamova:** Data curation (equal); Software (lead). **G. Gizer:** Investigation (supporting); Methodology (equal). **C. Pistidda:** Methodology (equal); Resources (equal); Writing-review-editing (supporting). **D. Renner:** Methodology (supporting). **H. Noei:** Investigation (supporting); Supervision (supporting); Writing-review-editing (supporting). **V. Vonk:** Investigation (supporting); Project administration (supporting); Resources (equal); Supervision (equal); Validation (supporting); Writing-review-editing (equal). **A. Stierle:** Conceptualization (equal); Funding acquisition (lead); Project administration (lead); Resources (equal); Supervision (equal); Validation (equal); Writing – review & editing (equal).

DATA AVAILABILITY

Raw data were generated at the PETRA III beamline P21.2 at DESY (Hamburg, Germany). Derived data supporting the findings of this study are available from the corresponding author upon reasonable request.

REFERENCES

[1] M. Salmeron, Top. Catal. **61**, 2044 (2018).
[2] C. Schlueter, A. Gloskovskii, K. Ederer, I. Schostak, S. Piec, I. Sarkar, Y. Matveyev, P. Lömker, M. Sing, R. Claessen, C. Wiemann, C. M. Schneider, K. Medjanik, G. Schönhense, P. Amann, A. Nilsson, and W. Drube, AIP Conf. Proc. **2054**, 040010 (2019).
[3] F. Tao, L. Nguyen, and S. Zhang, Rev. Sci. Instrum. **84**, 034101 (2013).
[4] R. V. Mom, W. G. Onderwaater, M. J. Rost, M. Jankowski, S. Wenzel, L. Jacobse, P. F. A. Alkemade, V. Vandalon, M. A. van Spronsen, M. van Weeren *et al.*, Ultramicroscopy **182**, 233 (2017).
[5] C. T. Herbschleb, P. C. Van Der Tuijn, S. B. Roobol, V. Navarro, J. W. Bakker, Q. Liu, D. Stoltz, M. E. Cañas-Ventura, G. Verdoes, M. A. Van Spronsen *et al.*, Rev. Sci. Instrum. **85**, 083703 (2014).
[6] V. Vonk and H. Graafsma, *In-situ Materials Characterization* (Springer, 2014), pp. 39–58.
[7] A. Stierle, J. Gustafson, and E. Lundgren, *Operando Research in Heterogeneous Catalysis* (Springer, 2017), pp. 59–87.
[8] P. Bernard, K. Peters, J. Alvarez, and S. Ferrer, Rev. Sci. Instrum. **70**, 1478 (1999).
[9] F. J. Wirkert, M. Paulus, J. Nase, J. Möller, S. Kujawski, C. Sternemann, and M. Tolan, J. Synchrotron Radiat. **21**, 76 (2014).
[10] F. Venturini, S. Schöder, W. F. Kuhs, V. Honkimäki, L. Melesi, H. Reichert, H. Schober, and F. Thomas, J. Synchrotron Radiat. **18**, 251 (2011).
[11] A. E. F. de Jong, V. Vonk, V. Honkimäki, B. Gorges, H. Vitoux, and E. Vlieg, J. Cryst. Growth **420**, 84 (2015).
[12] M. Bowker, ChemCatChem **11**, 4238 (2019).
[13] S. K. Matam, M. H. Aguirre, A. Weidenkaff, and D. Ferri, J. Phys. Chem. C **114**, 9439 (2010).
[14] B. A. Talagañis, F. J. Castro, A. Baruj, and G. Meyer, Rev. Sci. Instrum. **80**, 073901 (2009).
[15] B. R. S. Hansen, K. T. Møller, M. Paskevicius, A.-C. Dippel, P. Walter, C. J. Webb, C. Pistidda, N. Bergemann, M. Dornheim, T. Klassen, J.-E. Jørgensen, and T. R. Jensen, J. Appl. Crystallogr. **48**, 1234 (2015).
[16] U. Bösenberg, C. Pistidda, M. Tolkiehn, N. Busch, I. Saldan, K. Suarez-Alcantara, A. Arendarska, T. Klassen, and M. Dornheim, Int. J. Hydrogen Energy **39**, 9899 (2014).
[17] B. Clausen, J. Catal. **132**, 524 (1991).
[18] P. J. Chupas, K. W. Chapman, C. Kurtz, J. C. Hanson, P. L. Lee, and C. P. Grey, J. Appl. Crystallogr. **41**, 822 (2008).
[19] U. Hejral, D. Franz, S. Volkov, S. Francoual, J. Strempfer, and A. Stierle, Phys. Rev. Lett. **120**, 126101 (2018).
[20] S. Couet, T. Diederich, K. Schlage, and R. Röhlsberger, Rev. Sci. Instrum. **79**, 093908 (2008).
[21] G. Eres, C. M. Rouleau, Q. Lu, Z. Zhang, E. Benda, H. N. Lee, J. Z. Tischler, and D. D. Fong, Rev. Sci. Instrum. **90**, 093902 (2019).
[22] S. Pfaff, J. Zhou, U. Hejral, J. Gustafson, M. Shipilin, S. Albertin, S. Blomberg, O. Gutowski, A. Dippel, E. Lundgren, and J. Zetterberg, Rev. Sci. Instrum. **90**, 033703 (2019).
[23] D. Burkle, R. De Motte, W. Taleb, A. Kleppe, T. Comyn, S. M. Vargas, A. Neville, and R. Barker, Rev. Sci. Instrum. **87**, 105125 (2016).
[24] N. Aslan, C. Horstmann, O. Metz, O. Kotlyar, M. Dornheim, C. Pistidda, S. Busch, W. Lohstroh, M. Müller, and K. Pranzas, J. Neutron Res. **21**, 125 (2019).

[25]C. Chantler, K. Olsen, R. Dragoset, J. Chang, A. Kishore, S. Kotochigova, and D. Zucker, X-Ray Form Factor, Attenuation and Scattering Tables—NIST Standard Reference Database 66, 2005; accessed 6 October 2021.
[26]H. Reichert, V. Honkimäki, A. Snigirev, S. Engemann, and H. Dosch, Physica B **336**, 46 (2003).
[27]K. E. Petersen, Proc. IEEE **70**, 420 (1982).
[28]T. P. Trainor, P. J. Eng, and I. K. Robinson, J. Appl. Crystallogr. **35**, 696 (2002).
[29]See https://www.vareximaging.com/wp-content/uploads/2022/01/XRD-4343CT_118914-1.pdf for Varex Imaging XRD 4343CT Industrial Flat Panel Detector, © 2021 Varex Imaging Corporation; accessed 24 April 2022.
[30]I. K. Robinson, Phys. Rev. B **33**, 3830 (1986).
[31]U. Hejral, P. Müller, M. Shipilin, J. Gustafson, D. Franz, R. Shayduk, U. Rütt, C. Zhang, L. R. Merte, E. Lundgren *et al.*, Phys. Rev. B **96**, 195433 (2017).